Bubble formation in organic light-emitting diodes

L. S. Liao
Surface Physics Laboratory, Fudan University, Shanghai 200433 and Center Of Super-Diamond and Advanced Films (COSDAF) and Department of Physics and Materials Science, City University of Hong Kong, Hong Kong, People's Republic of China

J. He, X. Zhou, M. Lu, Z. H. Xiong, Z. B. Deng, and X. Y. Hou
Surface Physics Laboratory, Fudan University, Shanghai 200433, People's Republic of China

S. T. Lee[a)]
Center Of Super-Diamond and Advanced Films (COSDAF) and Department of Physics and Materials Science, City University of Hong Kong, Hong Kong, People's Republic of China

(Received 16 September 1998; accepted for publication 21 March 2000)

Bubbles in organic light-emitting diodes can be formed from gas release due to Joule heating effect at localized electrical shorts during operation, which could be simulated by a rapid thermal annealing. The gases in the bubbles consist of not only adsorbed moistures but also the decomposed organic species, which are detected *in situ* in an ultrahigh vacuum chamber. In the device of Al/*tris*-(8-hydroxyquinoline) aluminum (Alq/*N*,*N*′-diphenyl-*N*.*N*′-*bis*-{3-methylphenyl}-{1,1′biphenyl}-4,4′-diamine/indium tin oxide (ITO), the gases released from ITO surface were mainly of adsorbed moistures, while those released from the organic layers were of both the decomposed products from Alq and the trapped moistures. The decomposition of Alq could not be easily avoided if there were severe localized electrical shorts in the devices. © *2000 American Institute of Physics.* [S0021-8979(00)00613-7]

I. INTRODUCTION

Since Tang and Van Slyke's report on efficient electroluminescence (EL) at low voltages from organic light-emitting diodes (OLEDs),[1] there has been significant progress in the field of OLED.[2] Nevertheless, the operational instability of the devices is still a problem of much concern,[3–17] which greatly limits the lifetime of OLEDs and remains a major obstacle for the commercialization of OLEDs.

Morphological change in the form of bubbles at the interface of metal electrode/organic layer of OLEDs is one kind of operational instability, which occurs when OLED is under electrical bias.[12–16] The bubbles can cause the metal electrode to delaminate from the organic layer and cut off the pathway of carrier transportation in micrometer-sized areas. As a result, the electroluminescence efficiency and brightness of the device will be decreased. Eventually the device will fail. This is one of the prominent failure phenomena. The elevated cathode bubbles can be formed due to gas evolution from galvanic corrosion of Mg/Ag electrode and/or electrolysis of absorbed moistures.[12,13] The bubbles can also be formed in polymer light-emitting diodes due to Joule heating effect.[15] The gases in the bubbles were the electrochemical products of moistures—oxygen and hydrogen—as reported by Do *et al.*[12] However, bubble formation due to decomposition of organic materials has not yet been reported. In this study, we show that bubble formation in OLEDs is mainly due to Joule heating effect, and the gases filling in the bubbles are of decomposed organic species as well as the adsorbed moistures in the devices. Moreover, we show that bubble formation has at least two origins, one of which could be from indium tin oxide (ITO) surface mainly due to desorption of moistures, and the other could be from organic materials due to both decomposed species and moistures.

II. EXPERIMENT

The devices used in this study had the structure of Al/*tris*-(8-hydroxyquinoline) aluminum (Alq/*N*,*N*′-diphenyl*N*.*N*′-*bis*-{3-methylphenyl} -{1,1′-biphenyl} -4,4′-diamine (TPD)/ITO. The thicknesses of ITO, TPD, Alq, and Al were 25, 40, 40, and 100 nm, respectively. TPD and Alq were purified by sublimation before film deposition. The ITO coated glass substrate with a sheet resistance of 77 $\Omega/\square$ was cleaned by scrubbing in detergent, rinsing in de-ionized water, and then ultrasonically washing in acetone, alcohol, and de-ionized water, respectively, and finally N_2 blown dry. The OLEDs were fabricated by using vacuum deposition (at $\sim 2\times 10^{-5}$ Torr). Rapid thermal annealing of OLEDs was carried out in a quartz box with a N_2 flux of 5 l/min at different temperatures within 50–500 °C for 60 s. The schematic diagrams of the OLED samples are shown in Fig. 1. The structure in Fig. 1(a) is for regular EL operation, and that in Fig. 1(b) is for thermal treatment only. An Olympus BH-2 microscope was used for the observation of bubble formation, and a conventional quadruple mass spectrometer and a Finnigar Voyager Gas Chromatogram/Mass Spectra system were employed for gas analysis.

III. RESULTS AND DISCUSSION

A. Joule heating effect

As shown in Fig. 1(a), two zones, namely zones 1 and 2, should be mentioned, which are located physically right next

a)Author to whom correspondence should be addressed; electronic mail: apannale@cityu.edu.hk

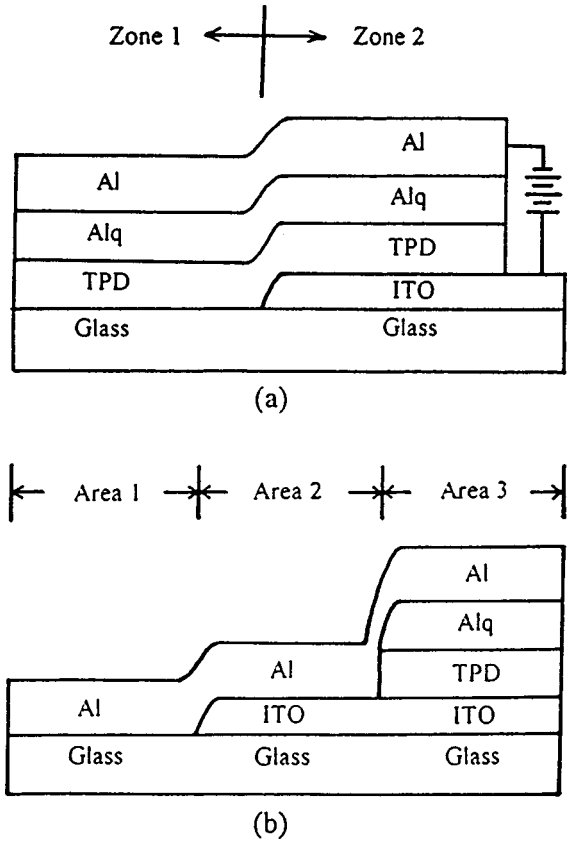

FIG. 1. Schematic diagrams of OLEDs used (a) for regular electrical operation and (b) for thermal treatment only.

to each other. The structure of zone 1 is Al/Alq/TPD (without ITO), and that of zone 2 is Al/Alq/TPD/ITO (device area). Before electric operation, both zone 1 and zone 2 were observed to have smooth morphology on the Al electrode surface. Obviously, no current could go through zone 1 under electrical bias because there is no ITO anode beneath the TPD layer. Therefore, when the sample was under forward bias, only zone 2 exhibited electroluminescence. During the experiment, we observed under optical microscope that some localized electrical shorts developed in zone 2 as the bias voltage increased, and many bubbles emerged around the shorts. Even after the voltage was switched off suddenly, we observed that some new bubbles continued to emerge on the Al electrode surface. Figure 2 is the morphological micrograph of a failed sample viewed from the side of Al electrode. It clearly shows that bubble formation has occurred in both zone 1 and zone 2 depicted in Fig. 1. Although no current could flow through zone 1, bubbles still were formed in this zone. This observation clearly shows that the bubble formation is not necessarily due to electrochemical or optoelectrochemical reactions in our experiment. Instead, the result suggests that the heat produced at the localized electrical shorts in zone 2 would propagate outwards to zone 1 nearby. The heating effect caused the effervescence of gas and thus formation of bubbles in both zones. We have also observed similar behavior of bubble formation at the boundary between the structures of Al/Alq and Al/Alq/ITO, which is shown in Fig. 3 as a further evidence of bubble formation caused by Joule heating.

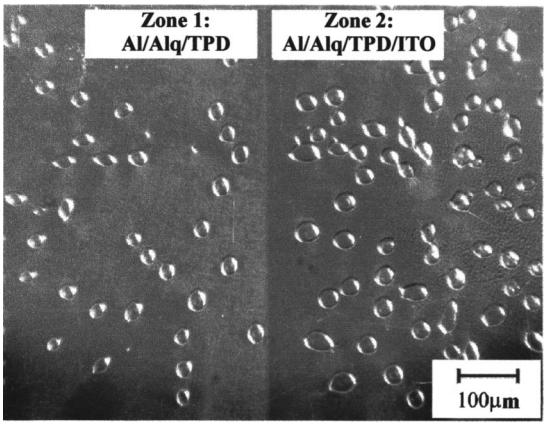

FIG. 2. Bubble formation in a failed device of Al/Alq/TPD/ITO. The layer structures [as shown in Fig. 1(a)] are zone 1: Al/Alq/TPD and zone 2: Al/Alq/TPD/ITO.

According to our measurement by infrared microscopy, the temperature in the center of some localized electrical shorts could be higher than 200 °C.[18] Although thermal annealing of our samples at 400 °C was found not to carbonize the organic film (see Sec. B below), carbonization could still take place at localized electrical shorts. This implies that the temperature at some localized electrical shorts might even be much higher than 200 °C. At temperatures much higher than 200 °C, adsorbed water and some organic species could be easily gasified. Therefore, bubble formation in OLEDs can indeed be formed due to Joule heating effect.

B. Bubble formation caused by thermal annealing

After establishing that bubble formation in OLEDs can be caused by Joule heating effect, we employ thermal treatment to simulate the failure process of OLEDs and to investigate the precursor and the composition of the released gases from specific locations. For this purpose, three different structures on different areas of a substrate shown in Fig. 1(b) were fabricated under the same deposition condition. The three areas were area 1: Al/glass; area 2: Al/ITO/glass; and area 3: Al/Alq/TPD/ITO/glass, respectively. The as-prepared

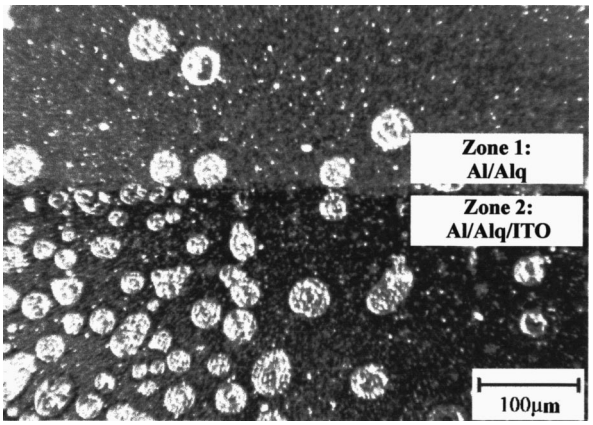

FIG. 3. Bubble formation in a failed device of Al/Alq/ITO. The layer structures are zone 1: Al/Alq and zone 2: Al/Alq/ITO. The picture was taken one day after device operation. Many bubbles were deformed due to gas contraction in these bubbles.

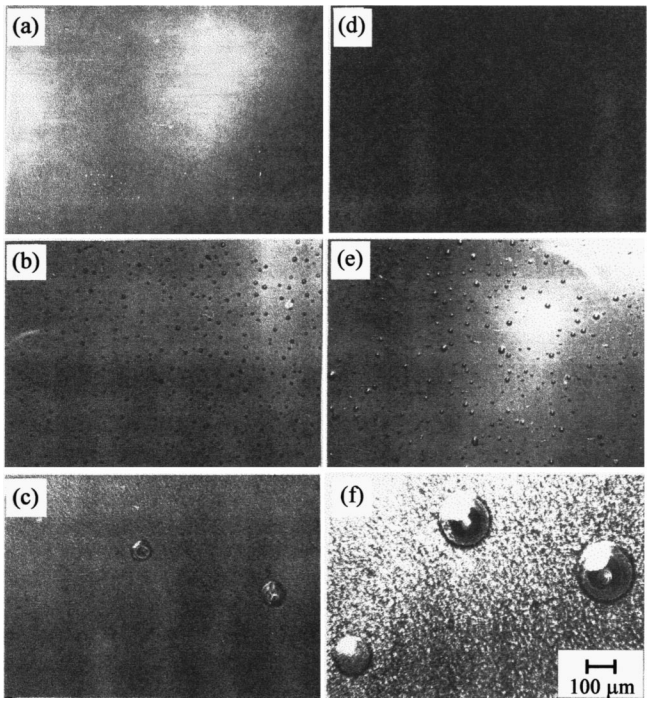

FIG. 4. Optical micrograph of the morphological changes in the OLED shown in Fig. 1(b). (a) and (d) refer to area 1 in Fig 1(b): Al/glass; (b) and (e) to area 2 in Fig 1(b): Al/ITO/glass; (c) and (f) to area 3 Fig. 1(b): Al/Alq/TPD/ITO/glass. (a), (b), and (c) were taken when the sample was treated by rapid thermal annealing in a quartz box with a N_2 flux of 5 l/min at 120 °C for 60 s; (d), (e), and (f) were taken at 400 °C and the other conditions were the same as above.

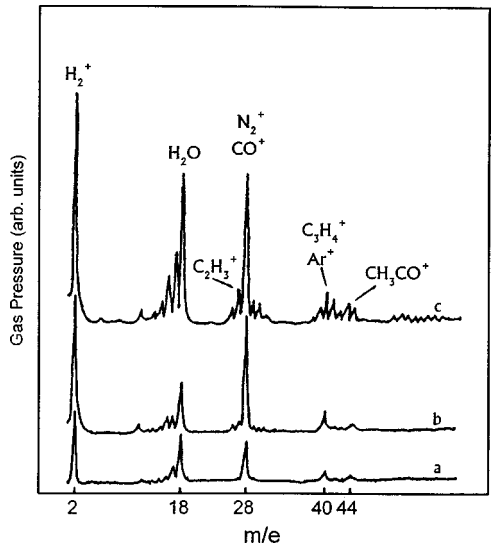

FIG. 5. Mass spectra obtained with the sample holder under thermal treatment; (a) background spectrum at room temperature and (b) background spectrum at 200 °C. (c) Mass spectrum obtained at 200 °C with the sample loaded with the ITO sample.

sample was then treated by rapid thermal annealing in a N_2 flux at different temperatures for 60 s. At 50 °C, no discernible morphological change in the three areas was observed under the optical microscope. At 80 °C bubbles were still not observed in any of the areas, but crystallization of organic layers took place in area 3. At 120 °C, no bubble was observed in area 1. A relatively high density of small bubbles of about 5 μm in diameter emerged in area 2, while a few bubbles with a diameter of more than 50 μm emerged in area 3. The morphology of the three areas annealed at 120 °C is shown in Figs. 4(a), 4(b), and 4(c), respectively. In addition to the bubble formation in Fig. 4(c), we also can see that crystallization has occurred in Fig. 4(c), which is expected to originate from TPD due to its lower glass transition temperature.[19] As the temperature increased further to 400 °C, again no bubble was observed in area 1. At 400 °C, the bubbles in area 2 did not change appreciably in size or in density, and the average bubble diameter was smaller than 10 μm. The density and size of the bubbles in area 3 increased gradually with increasing temperature, and their average diameter at 400 °C was about 100 μm, which is much bigger than that in area 2. The morphology of the three areas after annealing at 400 °C is shown in Figs. 4(d), 4(e), and 4(f), respectively. It is worth noting that no carbonization occurred in any of the areas.

As is known, metal electrode may be delaminated due to crystallization of organic materials,[8] or a difference in the thermal expansion coefficients between metal and organic materials. However, delamination could not have led to the formation of the big bubbles with a semispherical shape as seen here [the height of bubbles is nearly equal to the radius of its sphere according to our previous observation by scanning electron microscopy (SEM)], nor could it have caused the rupture bubbles. Similar to the report by Savvate'ev *et al.*,[15] we believe that the bubble formation in our work is caused by gas effervescence judging from the shape, size and expansion process of the bubbles. Therefore, the result from Fig. 4 reveals that gases could be released from both ITO and organic materials. The bubbles formed on the ITO surface are smaller in size but higher in density, whereas those formed from organic materials are bigger in size but lower in density.

In addition, we found that the thickness of the metal electrode had an effect on the bubble size and density. Under the same annealing or biasing condition, when the metal electrode is thinner, the bubbles formed in the structure of Al/Alq/TPD/ITO/glass are smaller in size but higher in density, and the bubbles are easily broken during gas expansion. When the metal electrode is thicker, the bubble size is bigger but density is lower, and the bubbles are not easily broken during gas expansion. Obviously, no bubble could be formed on the surface of samples without the covering metal electrode. It means that the released gases gather at the metal/organic interface and force the metal film to protrude locally, resulting in the formation of bubbles.

C. Chemical analysis of released gases

Figure 5 shows the mass spectra measured in an ultrahigh vacuum chamber (at $\sim 10^{-9}$ Torr). Curves (a) and curve (b) are the background spectra obtained with the sample holder empty at room temperature and at 200 °C, respectively. Next, a clean ITO-coated glass substrate was put in the sample holder and curve (c) was obtained with the sample holder heated to 200 °C. Intensive peaks of H_2^+ ($m/e=2$), H_2O^+ ($m/e=18$) and a few new peaks of or-

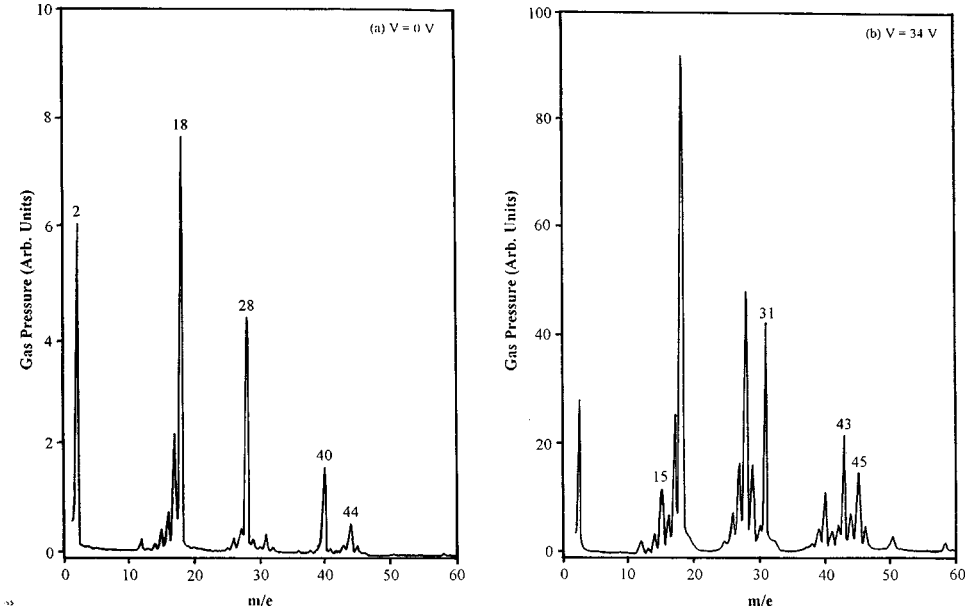

FIG. 6. Mass spectra of OLED sample under a forward bias of (a) 0 V and (b) 34 V.

ganic substances (probably the fragments from acetone and alcohol) are observed in curve (c). Comparing curves (c) and (b), it is obvious that the gases desorbed and released from the heated (ITO) surface were mainly moistures and some organic species, which were adsorbed on the surface during sample processing. Therefore, the small bubbles at the Al/ITO interface were filled mainly with moistures and some organic species.

The species adsorbed on the ITO surface could be readily removed by rapid thermal annealing (RTA) or plasma cleaning. Using an RTA-treated ITO glass substrate, we made a set of OLEDs similar to those shown in Fig. 1(b) to investigate the process of bubble formation. We found that in the sample made with the RTA-treated ITO no bubble at the Al/ITO interface [area 2 in Fig. 1(b)] was formed. However, big bubbles were still observed in area 3, and the bubbles also burst under a high electrical bias. The result shows that the gas released from organic materials has a more dominant influence on the bubble formation than the gas desorbed from ITO.

In situ mass spectra were measured from an OLED on a RTA-treated ITO substrate operating under a forward bias voltage (V) in an ultrahigh vacuum chamber (at $\sim 10^{-9}$ Torr). As the forward bias increased, the pressure in the chamber increased. Figures 6(a) and 6(b) are the spectra recorded with a bias of $V=0$ and 34 V, respectively. At 34 V, intense peaks of H_2O^+ ($m/e=18$), CH_2OH^+ ($m/e=31$), and $C_3H_7^+$ ($m/e=43$) emerged and were over one order of magnitude more intense than those at 0 V. It means that both moistures and organic gases are the dominant species released. The detected H_2O^+ peak may come from both the Al electrode surface and organic films, but the peaks of organic gases can only come from the organic films.

To identify the chemical nature of the gases released from the organic films, we performed analysis using gas chromatography in combination with mass spectral measurement in the range of $m/e>40$. We first peeled off the Al electrode from the top of the sample, and then dissolved the Alq and TPD films in CH_2Cl_2. Figure 7 shows the gas chromatogram from the resultant solution of Alq and TPD between the retention time (rt) from 4 to 18 min [the corresponding temperature (T) is from 40 to 250 °C approximately]. According to the mass spectral analysis, the solution first gave off some impurities, such as siloxane $C_6H_{18}O_3Si_3$, at $rt=4.909$ and $T\approx 55$ °C, and then some decomposed gases of Alq, such as oxyquinoline C_9H_7ON, at $rt=11.427$ and $T\approx 150$ °C. Therefore, it is revealed that the released organic gases from the organic films were mainly oxyquinoline and other impurities, which may be introduced during material synthesis. The result suggests that further purification of the organic materials is needed.

In view of the above gas analysis, we paid special attention to remove the adsorbates from the ITO surface, and made further purification of the Alq and TPD materials. However, bubbles still formed in the new OLEDs made with these precautions when the devices were heated to above 200 °C or operated under a forward bias. It means that Alq decomposition still took place in these OLEDs. Papadimitrakopoulos, Zhang, and Higginson[17] reported that Alq could be easily decomposed in the presence of water. This thus suggests that gas release due to decomposition of organic materials in OLEDs cannot be easily avoided unless adsorbed water and localized electrical shorts are eliminated.

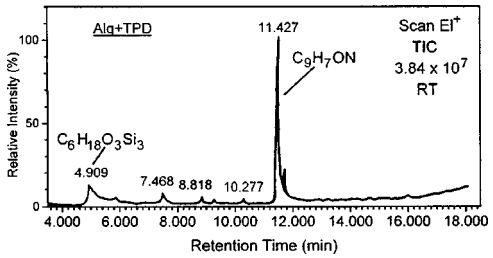

FIG. 7. Gas chromatogram of the solution containing dissolved Alq and TPD.

IV. CONCLUSION

It has been shown that bubble formation at the cathode/organic interface in OLEDs can be caused by Joule heating effect due to the localized electrical shorts during operation. This Joule heating effect could also be simulated by a rapid thermal annealing method. The gases in the bubbles could originate both from the decomposition of organic materials and from adsorbed moistures in the devices. The adsorbates on the ITO surface could be easily removed by thermal treatment before the deposition of organic layers. However, decomposition of organic materials could not be easily avoided due to localized Joule heating effect.

ACKNOWLEDGMENTS

The authors would like to express their thanks to Professor Xun Wang for his guidance. This work was partly supported by the National Natural Science Foundation of China under project No. 69776034 and by the Research Grant Council of Hong Kong (Nos. 9040293, 8730009, and 9040345).

[1] C. W. Tang and S. A. Van Slyke, Appl. Phys. Lett. **51**, 913 (1987).
[2] C. W. Tang, SID96 Digest, 181, Society for Information Display, 1996.
[3] P. E. Burrows, V. Bulovic, S. R. Forrest, L. S. Sapochak, D. M. McCarty, and M. E. Thompson, Appl. Phys. Lett. **65**, 2922 (1994).
[4] J. C. Scott, J. H. Kaufman, P. J. Brock, R. DiPietro, J. Salem, and J. A. Groitia, J. Appl. Phys. **79**, 2745 (1996).
[5] C. L. Chao, K. R. Chuang, and S. A. Chen, Appl. Phys. Lett. **69**, 2894 (1996).
[6] J. Shi and C. W. Tang, Appl. Phys. Lett. **70**, 1665 (1997).
[7] S. A. Carter, M. Angelopoulos, S. Karg, P. J. Brock, and J. C. Scott, Appl. Phys. Lett. **70**, 2067 (1997).
[8] H. Aziz, Z. Popovic, S. Xie, A. M. Hor, N. X. Hu, C. Tripp, and G. Xu, Appl. Phys. Lett. **72**, 756 (1998).
[9] B. H. Cumpston and K. F. Jensen, Appl. Phys. Lett. **69**, 3941 (1996).
[10] E. Gautier, A. Lorin, J. M. Nunzi, A. Schalchli, J. J. Benattar, and D. Vital, Appl. Phys. Lett. **69**, 1071 (1996).
[11] J. R. Sheats, H. Antoniadis, M. Hueschen, W. Leonard, J. Miller, R. Moon, D. Roitman, and A. Stocking, Science **273**, 884 (1996).
[12] L. M. Do, M. Oyamada, A. Koike, E. M. Han, N. Yamamoto, and M. Fujihira, Thin Solid Films **273**, 209 (1996).
[13] H. Aziz, Z. Popovic, C. P. Tripp, N. X. Hu, A. M. Hor, and G. Xu, Appl. Phys. Lett. **72**, 2642 (1998).
[14] J. McElvain, H. Antoniadis, M. R. Hueschen, J. N. Miller, D. M. Roitman, and R. L. Moon, J. Appl. Phys. **80**, 6002 (1996).
[15] V. N. Savvate'ev, A. V. Yakimov, D. Davidov, R. M. Pogreb, R. Neumann, and Y. Avny, Appl. Phys. Lett. **71**, 3344 (1997).
[16] L. M. Do, K. Kim, T. Zyung, H. K. Shim, and J. J. Kim, Appl. Phys. Lett. **70**, 3470 (1997).
[17] F. Papadimitrakopoulos, X.-M. Zhang, and K. A. Higginson, IEEE J. Sel. Top. Quantum Electron. **4**, 49 (1998).
[18] X. Zhou, J. He, L. S. Liao, M. Lu, X. M. Ding, X. Y. Hou, and S. T. Lee, Adv. Mater. **12**, 265 (2000).
[19] K. Naito and A. Miura, J. Phys. Chem. **97**, 6240 (1993).